

1     **Estimates of late middle Eocene pCO<sub>2</sub> based on stomatal density of**  
2                             **modern and fossil *Nageia* leaves**

3

4                             XIAO-YAN LIU, QI GAO, MENG HAN and JIAN-HUA JIN\*

5

6     State Key Laboratory of Biocontrol and Guangdong Provincial Key Laboratory of Plant Resources,  
7     School of Life Sciences, Sun Yat-sen University, Guangzhou 510275, China

8

9     **Abstract:**

10    Atmospheric pCO<sub>2</sub> concentrations have been estimated for intervals of the Eocene  
11    using various models and proxy information. Here we reconstruct late middle Eocene  
12    (42.0-38.5 Ma) pCO<sub>2</sub> based on the fossil leaves of *Nageia maomingensis* Jin et Liu  
13    collected from the Maoming Basin, Guangdong Province, China. We first determine  
14    relationships between atmospheric pCO<sub>2</sub> concentrations, stomatal density (SD) and  
15    stomatal index (SI) using “modern” leaves of *N. motleyi* (Parl.) De Laub, the nearest  
16    living species to the Eocene fossils. This work indicates that the SD inversely  
17    responds to pCO<sub>2</sub>, while SI has almost no relationship with pCO<sub>2</sub>. Eocene pCO<sub>2</sub>  
18    concentrations can be reconstructed based on a regression approach and the stomatal  
19    ratio method by using the SD. The first approach gives a pCO<sub>2</sub> of 351.9 ± 6.6 ppmv,  
20    whereas the one based on stomatal ratio gives a pCO<sub>2</sub> of 537.5 ± 56.5 ppmv. Here, we  
21    explored the potential of *N. maomingensis* in pCO<sub>2</sub> reconstruction and obtained

---

\*

Correspondence: Jianhua Jin, tel. +86 20 84113348, fax +86 20 84110436, e-mail: lssjhh@mail.sysu.edu.cn

22 different results according to different methods, providing a new insight for the  
23 reconstruction of paleoclimate and paleoenvironment in conifers.

24

25 **Keywords:** pCO<sub>2</sub>, late middle Eocene, *Nageia*, Maoming Basin, South China.

26

## 27 **1 Introduction**

28

29 The Eocene (55.8-33.9 Ma) generally was much warmer than present-day, although  
30 temperatures varied significantly across this time interval (Zachos et al., 2008).

31 Climate of the early Eocene was extremely warm, particularly during the early  
32 Eocene Climatic Optimum (EECO; 51 to 53 Ma), and the Paleocene-Eocene Thermal  
33 Maximum (PETM; ~55.9 Ma). However, global climatic conditions cooled  
34 significantly by the middle to late Eocene (40 to 36 Ma). Indeed, small, ephemeral  
35 ice-sheets and Arctic sea ice likely existed during the latest Eocene (Moran et al.,  
36 2006; Zachos et al., 2008).

37 Many authors have suggested that changes in temperature during the Phanerozoic  
38 were linked to atmospheric pCO<sub>2</sub> (Petit et al., 1999; Retallack, 2001; Royer, 2006).  
39 Central to these discussions are records across the Eocene, as this epoch spans the last  
40 major change from a “greenhouse” world to an “icehouse” world. The Eocene pCO<sub>2</sub>  
41 record remains incomplete and debated (Kürschner et al., 2001; Royer et al., 2001;  
42 Beerling et al., 2002; Greenwood et al., 2003; Royer, 2003). Most pCO<sub>2</sub>  
43 reconstructions have focused on the Cretaceous-Tertiary and Paleocene-Eocene

44 boundaries (65 to 50 Ma) and the middle Eocene. In particular, there are few  
45 reconstructions for the late middle Eocene (Pagani et al., 2005; Maxbauer et al., 2014).  
46 In addition, the pCO<sub>2</sub> reconstruction results have varied based on different proxies.  
47 Various methods having been used in pCO<sub>2</sub> reconstruction mainly include the  
48 computer modeling methods: GEOCARB-I, GEOCARB-II, GEOCARB-III,  
49 GEOCARB-SULF and the proxies: ice cores, paleosol carbonate, phytoplankton,  
50 nahcolite, Boron, and stomata parameters.

51 The abundance of stomatal cells can be measured on modern leaves and  
52 well-preserved fossil leaves. Various plants show a negative correlation between  
53 atmospheric CO<sub>2</sub> concentration and stomatal density (SD), stomatal index (SI), or  
54 both. As such, these parameters have been determined in fossil leaves to reconstruct  
55 past pCO<sub>2</sub>; examples include *Ginkgo* (Retallack, 2001, 2009a; Beerling et al., 2002;  
56 Royer, 2003; Kürschner et al., 2008; Smith et al., 2010), *Metasequoia* (Royer, 2003;  
57 Doria et al., 2011), *Taxodium* (Stults et al., 2011), *Betula* (Kürschner et al., 2001; Sun  
58 et al., 2012), *Neolitsea* (Greenwood et al., 2003), and *Quercus* (Kürschner et al., 1996,  
59 2001), *Laurus* and *Ocotea* (Kürschner et al., 2008). Recently, positive correlations  
60 between stomatal index or stomatal frequency and pCO<sub>2</sub> have been reported based on  
61 fossil *Typha* and *Quercus* (Bai et al., 2015; Hu et al., 2015). However, the tropical and  
62 subtropical moist broadleaf forest conifer tree *Nageia* has not been used previously in  
63 paleobotanical estimates of pCO<sub>2</sub> concentration.

64 Herein, we firstly document correlations between stomatal properties and  
65 atmospheric CO<sub>2</sub> concentrations using leaves of the extant species *Nageia motleyi*

66 (Parl.) De Laub. that were collected over the last two centuries. This provides a  
67 training dataset for application to fossil representatives of *Nageia*. We secondly  
68 measure stomatal parameters on fossil *Nageia* leaves from late middle Eocene of  
69 South China to estimate past CO<sub>2</sub> levels. The work provides further insights for  
70 discussing Eocene climate change.

71

## 72 **2 Background**

73

### 74 **2.1 Stomatal proxy in pCO<sub>2</sub> research**

75

76 Stomatal information gathered from careful examination of leaves has been widely  
77 used for reconstructions of past pCO<sub>2</sub> concentrations (Beerling and Kelly, 1997; Doria  
78 et al., 2011). The three main parameters are stomatal density (SD), which is expressed  
79 as the total number of stomata divided by area, epidermal density (ED), which is  
80 expressed as the total number of epidermal cells per area, and the stomatal index (SI),  
81 which is defined as the percentage of stomata among the total number of cells within  
82 an area [ $SI = SD \times 100 / (SD + ED)$ ]. Woodward (1987) considered that both SD and SI  
83 had inverse relationships with atmospheric CO<sub>2</sub> during the development of the leaves.  
84 Subsequently, McElwain (1998) created the stomatal ratio (SR) method to reconstruct  
85 pCO<sub>2</sub>. SR is a ratio of the stomatal density or index of a fossil [ $SD_{(f)}$  or  $SI_{(f)}$ ] to that of  
86 corresponding nearest living equivalent [ $SD_{(e)}$  or  $SI_{(e)}$ ], expressed as follows:

$$87 \quad SR = SI_{(e)} / SI_{(f)} \quad (1)$$

88 The stomatal ratio method is a semi-quantitative method of reconstructing pCO<sub>2</sub>  
 89 concentrations under certain standardizations. An example is the “Carboniferous  
 90 standardization” (Chaloner and McElwain, 1997), where one stomatal ratio unit  
 91 equals two RCO<sub>2</sub> units:

$$92 \quad SR = 2 \text{ RCO}_2 \quad (2)$$

93 and the value of RCO<sub>2</sub> is the pCO<sub>2</sub> level divided by the pre-industrial atmospheric  
 94 level (PIL) of 300 ppm (McElwain, 1998) or that of the year when the nearest living  
 95 equivalent (NLE) was collected (Berner, 1994; McElwain, 1998):

$$96 \quad \text{RCO}_2 = C_{(f)} / 300 \text{ or } \text{RCO}_2 = C_{(f)} / C_{(e)} \quad (3)$$

97 The estimated pCO<sub>2</sub> level can then be expressed as follows:

$$98 \quad C_{(f)} = 0.5 \times C_{(e)} \times SD_{(e)} / SD_{(f)} \text{ or } C_{(f)} = 0.5 \times C_{(e)} \times SI_{(e)} / SI_{(f)} \quad (4)$$

99 where  $C_{(f)}$  is the pCO<sub>2</sub> represented by the fossil leaf, and  $C_{(e)}$  is the atmospheric CO<sub>2</sub>  
 100 of the year when the leaf of the NLE species was collected (McElwain and Chaloner,  
 101 1995, 1996; McElwain 1998). The equation adapts to the pCO<sub>2</sub> concentration prior to  
 102 Cenozoic.

103 Another standardization, the “Recent standardization” (McElwain, 1998), is  
 104 expressed as one stomatal ratio unit being equal to one RCO<sub>2</sub> unit:

$$105 \quad SR = 1 \text{ RCO}_2 \quad (5)$$

106 According to the equations stated above, the pCO<sub>2</sub> concentration can be expressed  
 107 as:

$$108 \quad C_{(f)} = C_e \times SD_{(e)} / SD_{(f)} \text{ or } C_{(f)} = C_e \times SI_{(e)} / SI_{(f)} \quad (6)$$

109 This standardization is usually used for reconstruction based on Cenozoic fossils

110 (Chaloner and McElwain, 1997; McElwain, 1998; Beerling and Royer, 2002).  
111 Kouwenberg et al. (2003) proposed some special stomatal quantification methods  
112 for conifer leaves with stomata arranged in rows. The stomatal number per Length  
113 (SNL) is expressed as the number of abaxial stomata plus the number of adaxial  
114 stomata divided by leaf length in millimeters. Stomatal rows (SRO) is expressed as  
115 the number of stomatal rows in both stomatal bands. Stomatal density per length  
116 (SDL) is expressed as the equation  $SDL = SD \times SRO$ . True stomatal density per  
117 length (TSDL) is expressed as the equation  $TSDL = SD \times \text{band width (in millimeters)}$ .  
118 The band width on *Nageia motleyi* leaves was measured as leaf blade width.

119

## 120 **2.2 Review of extant and fossil *Nageia***

121

122 The genus *Nageia*, including seven living species, is a special group of  
123 Podocarpaceae, a large family of conifers mainly distributed in the southern  
124 hemisphere. *Nageia* has broadly ovate-elliptic to oblong-lanceolate, multiveined  
125 (without a midvein), spirally arranged or in decussate, and opposite or subopposite  
126 leaves (Cheng et al., 1978; Fu et al., 1999). Generally, *Nageia* is divided into two  
127 sections, *Nageia* Sect. *Nageia* and *Nageia* Sect. *Dammaroideae* (Mill 1999, 2001).  
128 Both sections are mainly distributed in southeast Asia and Australasia from north  
129 latitude 30° to nearly the equator (Fu, 1992; Fig. 1). Four species of the *N.* section  
130 *Nageia* -- *Nageia nagi* (Thunberg) O. Kuntze, *N. fleuryi* (Hickel) De Laub., *N.*  
131 *formosensis* (Dummer) C. N. Page, and *N. nankoensis* (Hayata) R. R. Mill -- have

132 hypostomatic leaves where stomata only occur on the abaxial side. One species of this  
133 section -- *N. maxima* (De Laub.) De Laub. -- is characterized by amphistomatic leaves,  
134 but where only a few stomata are found on the adaxial side (Hill and Pole, 1992; Sun,  
135 2008). Both *N. wallichiana* (Presl) O. Kuntze and *N. motleyi* of the *N.* section  
136 *Dammaroideae* are amphistomatic with abundant stomata distributed on both sides of  
137 the leaf. This is especially true for *N. motleyi*, which has approximately equal stomata  
138 numbers on both surfaces (Hill and Pole, 1992; Sun, 2008).

139 The fossil record of *Nageia* can be traced back to the Cretaceous. Krassilov (1965)  
140 described *Podocarpus (Nageia) sujfunensis* Krassilov from the Lower Cretaceous of  
141 Far East Russia. Kimura et al. (1988) reported *Podocarpus (Nageia) ryosekiensis*  
142 Kimura, Ohanaet Mimoto, an ultimate leafy branch bearing a seed, from the Early  
143 Barremian in southwestern Japan. In China, a Cretaceous petrified wood, *Podocarpus*  
144 (*Nageia*) *nagi* Pilger, was discovered from the Dabie Mountains in central Henan,  
145 China (Yang et al., 1990). Jin et al. (2010) reported a upper Eocene *Nageia* leaf  
146 named *N. hainanensis* Jin, Qiu, Zhu et Kodrul from the Changchang Basin of Hainan  
147 Island, South China. Recently, Liu et al. (2015) found another leaf species *N.*  
148 *maomingensis* Jin et Liu from upper middle Eocene of Maoming Basin, South China.  
149 Although some of the *Nageia* fossil materials described in the above studies  
150 (Krassilov, 1965; Jin et al., 2010; Liu et al., 2015) have well-preserved cuticles, these  
151 studies are mainly concentrated on morphology, systematics and phytogeography.

152 Here we try to reconstruct the pCO<sub>2</sub> concentration based on stomatal data of  
153 *Nageia maomingensis* Jin et Liu. Among the modern *Nageia* species mentioned above,

154 *N. motleyi* was considered as the NLE species of *N. maomingensis* (Liu et al., 2015).  
155 However, because of the species-specific inverse relationship between atmospheric  
156 CO<sub>2</sub> partial pressure and SD (Woodward and Bazzaz, 1988), it is necessary to explore  
157 whether the SD and SI of *N. motleyi* show negative correlations with the CO<sub>2</sub>  
158 concentration before applying the stomatal method. Both *N. maomingensis* and *N.*  
159 *motleyi* are amphistomatic, suggesting that both upper and lower surfaces of leaves  
160 might be used to estimate the pCO<sub>2</sub> concentrations.

161

### 162 **3 Material and methods**

163

#### 164 **3.1 Extant leaf preparation**

165

166 We examined 12 specimens of extant *Nageia motleyi* from different herbaria (Table  
167 1). We removed one or two leaves from each specimen, and took three fragments  
168 (0.25 mm<sup>2</sup>) from every leaf (Fig. 2a) and numbered them for analysis.

169 The numbered fragments were boiled for 5-10 min in water. Subsequently, after  
170 being macerated in a mixed solution of 10% acetic acid and 10% H<sub>2</sub>O<sub>2</sub> (1:1) and  
171 heated in the thermostatic water bath at 85 C for 8.5 hours, the reaction was stopped  
172 when the specimen fragments turned white and semitransparent. The cuticles were  
173 then rinsed with distilled water until the pH of the water became neutral. After, the  
174 cuticles were treated in Schulze's solution (one part of potassium chlorate saturated  
175 solution and three part of concentrated nitric acid) for 30 min, rinsed in water, and



176 then treated with 8% KOH (up to 30 min). The abaxial and adaxial cuticles were  
177 separated with a hair mounted on needle. Finally, the cuticles were stained with 1%  
178 Safranin T alcoholic solution for 5 min, sealed with Neutral Balsam and observed  
179 under LM.

180

### 181 **3.2 Fossil leaf preparation**

182

183 Maoming Basin (21°42'33.2"N, 110°53'19.4"E) is located in southwestern  
184 Guangdong, South China including Cretaceous and Tertiary strata. Tertiary strata are  
185 fluvial and lacustrine sedimentary units, divided into the Gaopengling, Laohuling,  
186 Shangcun, Huangniuling and Youganwo formations in descending order, aged from  
187 late Eocene to early Oligocene (Wang et al., 1994).

188 Four fossil leaves of *Nageia maomingensis* were recovered from the Youganwo  
189 (MMJ1-001) and Huangniuling (MMJ2-003, MMJ2-004 and MMJ3-003) formations  
190 of Maoming Basin, South China. Further information on the sections is provided by  
191 Liu et al. (2015). Importantly, the formations span a depositional age of  
192 approximately 42.0 to 38.5 Ma which was considered as late Eocene by Wang et al.  
193 (1994), but it can be recognized as late middle Eocene according to Walker and  
194 Geissman (2009).

195 Macrofossil cuticular fragments were taken from the middle part of each fossil leaf  
196 (Fig. 2c) and directly treated with Schulze's solution for approximately 1h and 5–10%  
197 KOH for 30 min (Ye, 1981). The cuticles were observed and photographed under a

198 Carl Zeiss Axio Scope A1 light microscope (LM). All fossil specimens and cuticle  
199 slides are housed in the Museum of Biology of Sun Yat-sen University, Guangzhou,  
200 China.

201

### 202 **3.3 Stomatal counting strategy and calculation methods**

203

204 The basic stomatal parameters, SD, ED and SI, were counted based on analyzing  
205 pictures taken with a light microscope (LM). A total of 2816 pictures (200×  
206 magnification of Zeiss LM) of cuticles from 21 leaves of *N. motleyi* were counted.  
207 Each counting field was 0.366 mm<sup>2</sup>. We used a standard sampling protocol (Poole and  
208 Kürschner, 1999), counting all full stomata in the image plus stomata straddling the  
209 left and top margins, as presented in Figure 2(b), and (d).

210 The SNL, SRO, SDL, and TSDL were also determined based on LM images. A  
211 total of 2293 pictures (200× magnification of Zeiss LM) of the cuticles from 21 leaves  
212 of *N. motleyi* were counted. Each counting field was 0.366 mm<sup>2</sup>. None of the  
213 aforementioned counting areas overlapped and they were larger than the minimum  
214 area (0.03 mm<sup>2</sup>) for statistics (Poole and Kürschner, 1999). In this study, the stomatal  
215 data of both surfaces are applied in pCO<sub>2</sub> reconstruction because both the fossil and  
216 NLE species are amphistomatic.

217

## 218 **4 Results**

219

220 **4.1 Correlations between the CO<sub>2</sub> concentrations and stomatal parameters of**

221 *Nageia motleyi*

222

223 The SD and SI data of the adaxial sides of *N. motleyi* leaves are presented in Table  
224 2. The SDs and SIs average 62.28 mm<sup>-2</sup> and 3.30 %, respectively. However, the SDs  
225 and SIs data of the abaxial sides, summarized in Table 3, give higher average values  
226 (70.03 mm<sup>-2</sup> in SDs and 3.90 % in SIs) than those from the adaxial sides. The  
227 combined SD and SI of the adaxial and abaxial surfaces average 66.14 mm<sup>-2</sup> and  
228 3.60 %, respectively (table 4).

229 Figure 3 shows the relationships between the stomatal parameters (SD and SI) of  
230 modern *N. motleyi* and the atmospheric CO<sub>2</sub> concentration (SD-CO<sub>2</sub> relationship and  
231 SI-CO<sub>2</sub> relationship). R<sup>2</sup> values in the SD-CO<sub>2</sub> relationship from the adaxial and  
232 abaxial surfaces of *N. motleyi* are up to 0.4667 and 0.3824 (Fig. 3a, b), suggesting that  
233 the stomatal densities of *N. motleyi* are inverse to the CO<sub>2</sub> concentrations. However,  
234 Fig. 3c and d indicate no relationship between the SIs and CO<sub>2</sub> concentrations for the  
235 extremely low level of the R<sup>2</sup> values (0.2558 and 0.0248). Figs. 3e and 3f based on the  
236 combined data also show that SD inversely responds to the atmospheric CO<sub>2</sub>  
237 concentration (R<sup>2</sup> = 0.4421), while SI has almost no relationship with the atmospheric  
238 CO<sub>2</sub> concentration (R<sup>2</sup> = 0.1177).

239 The mean values of SNL, SDL and TSDL are 9.81, 326.39 and 1226.93 no.·mm<sup>-1</sup>,  
240 respectively (Table 5). Fig. 4 shows the relationships between SNL (SDL, TSDL) and  
241 CO<sub>2</sub> concentrations. The low R<sup>2</sup> values in the Fig. 4a and 4c indicate that SNL (R<sup>2</sup> =

242 0.0643) and TSDL ( $R^2 = 0.0788$ ) have no relationship with the CO<sub>2</sub> concentration in  
243 this study. Fig. 4b shows that there is a weak reverse relevance between SDL and the  
244 CO<sub>2</sub> concentration ( $R^2 = 0.3154$ ).

245 Compared with the SDL method, the SD-based method shows a larger  $R^2$  value,  
246 indicating a stronger relevance between the SD and CO<sub>2</sub> concentrations. In this study,  
247 the pCO<sub>2</sub> is reconstructed based on the regression equations of SD-CO<sub>2</sub> relationship.  
248 Additionally, the stomatal ratio method can be also used in estimating pCO<sub>2</sub>  
249 concentration of late middle Eocene based on stomatal densities (SDs) of the fossil  
250 species *N. maomingensis* and extant species *N. motleyi*. The SD results of specimen  
251 No. 18328 are selected to reconstruct the pCO<sub>2</sub> concentration, because they are closest  
252 to the fitted equations in Fig. 3. This specimen was collected by Neth. Ind. For.  
253 Service from Riau on Ond. Karimon, Archipel. Ind., Malaysia, in 1934 at an altitude  
254 of 5 m and CO<sub>2</sub> concentration of 306.46 ppmv (Brown, 2010).

255

## 256 **4.2 The pCO<sub>2</sub> estimates results**

257

### 258 4.2.1 The regression approach

259 The summary of stomatal parameters of the fossil *Nageia* and reconstruction results  
260 are provided in Tables 6–8. The mean SD and SI values of the adaxial surface are 44.5  
261 mm<sup>-2</sup> and 1.8 %, respectively (Table 6). The mean SD and SI values of the abaxial  
262 surface are 49.8 mm<sup>-2</sup> and 2.07 %, respectively (Table 7).

263 Based on the regression approach, the pCO<sub>2</sub> was reconstructed as 351.9 ± 6.6 ppmv

264 and  $365.6 \pm 7.6$  ppmv according to the SD of adaxial and abaxial sides. The combined  
265 SD value is an average of  $46.6 \text{ mm}^{-2}$  (Table 8), giving the reconstructed pCO<sub>2</sub> of  
266  $358.1 \pm 5.0$  ppmv.

267

#### 268 4.2.2 The stomatal ratio method

269 Mean SR value of the adaxial side (SR= $1.69 \pm 0.18$ ) is a little larger than that of the  
270 abaxial side (SR= $1.60 \pm 0.11$ ) in fossil *Nageia* leaves (Tables 6 and 7). The pCO<sub>2</sub>  
271 reconstruction results are  $537.5 \pm 56.5$  ppmv (Table 6) and  $496.1 \pm 35.7$  ppmv (Table 7)  
272 based on the adaxial and abaxial cuticles, respectively. Based on the combined SD of  
273 both leaf sides, the pCO<sub>2</sub> result is  $519.9 \pm 35.0$  ppmv.

274 The partial pressure of CO<sub>2</sub> decreases with elevation (Gale, 1972). Jones (1992)  
275 proposed that the relationship between elevation and partial pressure in the lower  
276 atmosphere can be expressed as  $P = -10.6E + 100$ , where  $E$  is elevation in kilometers  
277 and  $P$  is the percentage of partial pressure relative to sea level. Various studies  
278 corroborate that SI and SD of many plants have positive correlations with altitude  
279 (Körner and Cochrane, 1985; Woodward, 1986; Woodward and Bazzaz, 1988;  
280 Beerling et al., 1992; Rundgren and Beerling, 1999) while they are negatively related  
281 to the partial pressure of CO<sub>2</sub> (Woodward and Bazzaz, 1988). Therefore, it is essential  
282 to take elevation calibration into account during pCO<sub>2</sub> concentration estimates.  
283 However, Royer (2003) pointed out that it is unnecessary to provide this conversion  
284 when trees lived at <250 m in elevation. In this paper, the nearest living equivalent  
285 species, *Nageia motleyi*, grows at 5 m in elevation with  $P = 99.9$ , suggesting that CO<sub>2</sub>

286 concentration estimates were only underestimated by 0.1%. Consequently, no  
287 correction is needed for the reconstruction result in this study. After being projected  
288 into a long-term carbon cycle model (GEOCARB III; Berner and Kothavalá 2001),  
289 the results of this study compares well with CO<sub>2</sub> concentrations for corresponding age  
290 within their error ranges (Fig. 5).

291

## 292 **5 Discussion**

293

### 294 **5.1 Stomatal parameters response to CO<sub>2</sub>**

295

296 For modern *Nageia*, we find that SD decreases as atmospheric CO<sub>2</sub> concentrations  
297 increase, but that SI does not. Generally, SI is more sensitive in response to the  
298 atmospheric CO<sub>2</sub> concentration than SD (Beerling, 1999; Royer, 2001). However, the  
299 reverse case has been observed for some flora. For example, Kouwenberg et al. (2003)  
300 reported that SD is better than SI in reflecting the negative relationships with CO<sub>2</sub> in  
301 conifer needles, accounting for the special paralleled mode of the ordinary epidermal  
302 and stomatal formation. Although *Nageia* is broad-leaved rather than needle-leaved, it  
303 also has well paralleled epidermal cells.

304 Compared with SD, the SDL has weaker correlation with CO<sub>2</sub> at a smaller R<sup>2</sup>. The  
305 SNL and TSDL have no response to the change of CO<sub>2</sub>. The insensitivity of SNL,  
306 SDL and TSDL might account for the characters of broad-leaved leaf shape and  
307 paralleled epidermal cells. The SNL should be applied to conifer needles with single

308 file of stomata (Kouwenberg et al., 2003). The SDL and TSDL were considered as the  
309 most appropriate method when the stomatal rows grouped in bands in a hypo- or  
310 amphistomatal conifer needle species (Kouwenberg et al., 2003). Considering all the  
311 stomatal parameters above, SD appears to be the most sensitive to CO<sub>2</sub>.

312 The SD-CO<sub>2</sub> correlation shows one value from leaf No. 40798 offset from the  
313 others. The SI-CO<sub>2</sub> correlation shows different offset values in different leaf sides.  
314 The offset values might be affected by leaf maturity and light intensity. However, it is  
315 hard to distinguish whether a fossil leaf was young or mature, or grew in a sunny or  
316 shady environment.

317 The R<sup>2</sup> value (0.5) of SD-CO<sub>2</sub> based on the adaxial side is higher than from the  
318 abaxial side and the combination of both sides, indicating that the correlation of  
319 SD-CO<sub>2</sub> is stronger than the others parameters herein. Therefore, the SD on the  
320 adaxial side is the best in reconstructing pCO<sub>2</sub>. The reconstruction result based on the  
321 regression approach is 351.9 ± 6.6 ppmv lower than the one based on the stomatal  
322 ratio method (Table 6), and it is relatively lower than the results based on the other  
323 proxies (Fig. 6; Freeman and Hayes, 1992; Pagani et al., 2005; Maxbauer et al., 2014).  
324 However, the result based on stomatal ratio method is 537.5 ± 56.5 ppmv, which is  
325 fairly close to GEOCARB III predictions (Fig. 5) and historical reconstruction trends  
326 (Fig. 6).

327

## 328 **5.2 Paleoclimate reconstructed history**

329

330 The pCO<sub>2</sub> levels throughout the Cenozoic were generally lower than during much  
331 of the Cretaceous, but probably also decreased significantly from the early to late  
332 Eocene. However, there is a wide range of estimates for the Eocene (Koch et al., 1992;  
333 Sinha and Stott, 1994; Ekart et al., 1999; Greenwood et al., 2003; Royer, 2003; Pagani  
334 et al., 2005; Wing et al., 2005; Lowenstein and Demicco, 2006; Fletcher et al., 2008;  
335 Zachos et al., 2008; Beerling et al., 2009; Bijl et al., 2010; Smith et al., 2010; Doria et  
336 al., 2011; Kato et al., 2011; Maxbauer et al., 2014).

337 Smith et al. (2010) reconstructed the value of the early Eocene pCO<sub>2</sub> ranging from  
338 580 ± 40 to 780 ± 50 ppmv using the stomatal ratio method (recent standardization)  
339 based on both SI and SD. A climatic optimum occurred in the middle Eocene  
340 (MECO): the reconstructed CO<sub>2</sub> concentrations are mainly between 700 to 1000  
341 ppmv during the late middle Eocene climate transition (42–38 Ma) using stomatal  
342 indices of fossil *Metasequoia* needles, but concentrations declined to 450 ppmv  
343 toward the top of the investigated section (Doria et al., 2011). Jacques et al. (2014)  
344 used CLAMP to calibrate climate change in Antarctica during the early-middle  
345 Eocene, suggesting a seasonal alternation of high- and low-pressure systems over  
346 Antarctica during the early-middle Eocene. Spicer et al. (2014) also reconstructed a  
347 relatively lower cool temperature than δ<sup>18</sup>O records (Keating-Bitonti et al., 2011) in  
348 the middle Eocene of Hainan Island, South China using CLAMP, indicating a not  
349 uniformly warm climate in the low latitude during the Eocene. An overall decreasing  
350 trend of the pCO<sub>2</sub> level was presented after the middle Eocene (Fig. 6; Retallack,  
351 2009b). The ice-sheets started to appear in the Antarctic during the Late Eocene



352 (Zachos et al., 2001), then the temperature suffered an apparent further decrease from  
353 the late Eocene onwards (Fig. 6).

354 In conclusion, although various results were made by different pCO<sub>2</sub> reconstruction  
355 proxies at the same time, their entire decreasing tendency of pCO<sub>2</sub> level are  
356 remarkably consistent with each other since the Eocene (Fig. 6). Fig. 6 shows that  
357 during the Eocene the temperature was higher than at present. Comparing to the  
358 estimates of late middle Eocene pCO<sub>2</sub> by Doria et al. (2011), the present result of  
359  $351.9 \pm 6.6$  ppmv based on the regression approach shows a remarkably lower pCO<sub>2</sub>  
360 level, while the one based on the stomatal ratio method of  $537.5 \pm 56.5$  ppmv is  
361 within the variation range of 500–1000 ppmv, which is closely consistent with the  
362 pCO<sub>2</sub> changes over the geological ages (Fig. 6). The world was dynamic in the  
363 Paleogene, including in the late middle Eocene, when the MECO occurred. Thus, the  
364 exact age matters, and it is possible that the values may differ because of slight offsets  
365 in time.

366

## 367 **6 Conclusion**

368

369 In this study, we reconstructed late middle Eocene pCO<sub>2</sub> based on the fossil leaves  
370 of *Nageia maomingensis* Jin et Liu from late middle Eocene of Maoming Basin,  
371 Guangdong Province, China. *Nageia* is a special element in conifers by its broad  
372 multi-veined leaf that lacks mid-vein. The stomatal data analysis suggests that only  
373 stomatal densities (SD) from both sides of *Nageia motleyi* leaves have significant

374 negative correlations with the atmospheric CO<sub>2</sub> concentration. The SD from the  
375 adaxial side gives the best correlation to the CO<sub>2</sub>. Based on SDs, the pCO<sub>2</sub>  
376 concentration is reconstructed using both the regression approach and the stomatal  
377 ratio method. The pCO<sub>2</sub> result based on the regression approach is 351.9 ± 6.6 ppmv,  
378 showing a relatively lower CO<sub>2</sub> level. The reconstructed result based on the stomatal  
379 ratio method is 537.5 ± 56.5 ppmv consistent with the variation trends based on the  
380 other proxies. Here, we explored the potential of *N. maomingensis* in pCO<sub>2</sub>  
381 reconstruction and obtained different results according to different methods, providing  
382 a new insight for the reconstruction of paleoclimate and paleoenvironment in conifers.

383

384 *Acknowledgements.* This study was supported by the National Natural Science  
385 Foundation of China (Grant No. 41210001, 41572011), and the Fundamental  
386 Research Funds for the Central Universities. We greatly thank the Herbarium of the  
387 V.L. Komarov Botanical Institute of the Russian Academy of Sciences (LE) for the  
388 permission to examine and collect extant *Nageia* specimens. We also express sincere  
389 gratitude to Prof. Sun Tongxing (Yancheng Teachers University), Dr. David Boufford  
390 (Harvard University) and Dr. Richard Chung Cheng Kong (Forest Research Institute  
391 Malaysia) for providing extant *N. motleyi* leaves from the herbarium of the Royal  
392 Botanic Garden at Edinburgh (E), the Harvard University Herbaria (A/GH) and the  
393 herbarium of Forest Research Institute Malaysia (KEP). We sincerely appreciate the  
394 guidance of Chengqian Wang (Harbin Institute of Technology) on preparing Figs. 3–6.  
395 We also offer sincere gratitude to Prof. Steven R. Manchester and Mr. Terry Lott

396 (Florida Museum of Natural History, University of Florida) for suggestions and  
397 modification.

398 **References**

- 399 Bai, Y. J., Chen, L. Q., Ranhotra, S. P., Wang, Q., Wang, Y. F., Li, C. S.:  
400 Reconstructing atmospheric CO<sub>2</sub> during the Plio–Pleistocene transition by fossil  
401 *Typha*. *Global Change Biology*, 21, 874–881, doi:10.1111/gcb.12670, 2015.
- 402 Beerling, D. J.: Stomatal density and index: theory and application, in: Jones, T. P.,  
403 and Rowe, N. P., (Eds.), *Fossil Plants and Spores: Modern Techniques*,  
404 Geological Society, London, 251–256, 1999.
- 405 Beerling, D. J., and Kelly, C. K.: Stomatal density responses of temperate woodland  
406 plants over the past seven decades of CO<sub>2</sub> increase: A comparison of salisbury  
407 (1927) with contemporary data, *American Journal of Botany*, 84, 1572–1583,  
408 1997.
- 409 Beerling, D. J., and Royer, D. L.: Reading a CO<sub>2</sub> signal from fossil stomata, *New*  
410 *Phytologist*, 153, 387–397, doi:10.1046/j.0028-646X.2001.00335.x, 2002.
- 411 Beerling, D. J., and Royer, D. L.: Convergent Cenozoic CO<sub>2</sub> history, *Natural*  
412 *Geoscience*, 4, 418–420, doi:10.1038/ngeo1186, 2011.
- 413 Beerling, D. J., Chaloner, W. G., Huntley, B., Pearson, J. A., Tooley, M. J., and  
414 Woodward, F. I.: Variations in the stomatal density of *Salix herbacea* L. under  
415 the changing atmospheric CO<sub>2</sub> concentrations of late- and post-glacial time,  
416 *Philosophical Transactions of the Royal Society of London*, ser. B. 336, 215–224,  
417 doi:10.1098/rstb.1992.0057, 1992.
- 418 Beerling, D. J., Fox, A., and Anderson, C. W.: Quantitative uncertainty analyses of  
419 ancient atmospheric CO<sub>2</sub> estimates from fossil leaves, *American Journal of*

420 Science, 309, 775–787, doi:10.2475/09.2009.01, 2009.

421 Beerling, D. J., Lomax, B. H., Royer, D. L., Upchurch Jr., G. R., and Kump, L. R.: An  
422 atmospheric  $p\text{CO}_2$  reconstruction across the Cretaceous-Tertiary boundary from  
423 leaf megafossils, Proceedings of the National Academy of Sciences of the United  
424 States of America, 99, 7836–7840, doi:10.1073/pnas.122573099, 2002.

425 Berner, R. A.: GEOCARB II: A revised model of atmospheric  $\text{CO}_2$  over Phanerozoic  
426 time, American Journal of Science, 294, 56–91, doi:10.2475/ajs.294.1.56, 1994.

427 Berner, R. A., and Kothavalá Z.: GEOCARB III: A revised model of Atmospheric  
428  $\text{CO}_2$  over Phanerozoic time, American Journal of Science, 301, 182–204,  
429 doi:10.2475/ajs.301.2.182, 2001.

430 Bijl, P. K., Houben, A. J. P., Schouten, S., Bohaty, S. M., Sluijs, A., Reichert, G.,  
431 Sinninghe Damsté J. S., and Brinkhuis, H.: Transient Middle Eocene  
432 atmospheric  $\text{CO}_2$  and temperature variations, Science, 330, 819–821,  
433 doi:10.1126/science.1193654, 2010.

434 Brown, L. R.: Atmospheric carbon dioxide concentration, 1000-2009 (Supporting  
435 data), in: Brown, L. R., (Ed.), World on the Edge: How to Prevent Environmental  
436 and Economic Collapse. Chapter 4 Data: Rising Temperatures, Melting Ice, and  
437 Food Security, Earth policy institute, Norton, W.W. & Company, New York,  
438 London ([http://www.earth-policy.org/books/wote/wote\\_data](http://www.earth-policy.org/books/wote/wote_data)), 2010.

439 Cerling, T. E.: Use of carbon isotopes in paleosols as an indicator of the  $P(\text{CO}_2)$  of the  
440 paleoatmosphere, Global Biogeochemical Cycles, 6, 307–314,  
441 doi:10.1029/92GB01102, 1992.

442 Chaloner, W. G., and McElwain, J. C.: The fossil plant record and global climate  
443 change, *Review of Palaeobotany and Palynology*, 95, 73–82,  
444 doi:10.1016/S0034-6667(96)00028-0, 1997.

445 Cheng, W. C., Fu, L. K., and Chao, C. S.: *Podocarpus* (Podocarpaceae), in: Cheng,  
446 Wanch ün, and Fu, Likuo, (Eds.), *Flora of China*, Science Press, Beijing, 7,  
447 398–422, 1978 (in Chinese).

448 Doria, G., Royer, D. L., Wolfe, A. P., Fox, A., Westgate, J. A., and Beerling, D. J.:  
449 Declining atmospheric CO<sub>2</sub> during the Late Middle Eocene climate transition,  
450 *American Journal of Science*, 311, 63–75, doi:10.2475/01.2011.03, 2011.

451 Ekart, D. D., Cerling, T. E., Montanez, I. P., and Tabor, N. J.: A 400 million year  
452 carbon isotope record of pedogenic carbonate: implications for paleoatmospheric  
453 carbon dioxide, *American Journal of Science*, 299, 805–827,  
454 doi:10.2475/ajs.299.10.805, 1999.

455 Fletcher, B. J., Brentnall, S. J., Anderson, C. W., Berner, R. A., and Beerling, D. J.:  
456 Atmospheric carbon dioxide linked with Mesozoic and Early Cenozoic climate  
457 change, *Nature Geoscience*, 1, 43–48, doi:10.1038/ngeo.2007.29, 2008.

458 Freeman, K. H., and Hayes, J. M.: Fractionation of carbon isotopes by phytoplankton  
459 and estimates of ancient CO<sub>2</sub> levels, *Global Biogeochemical Cycles*, 6, 185–198,  
460 doi:10.1029/92GB00190, 1992.

461 Fu, D. Z.: Nageiaceae – a new gymnosperm family, *Acta Phytotaxonomica Sinica*, 30,  
462 515–528, 1992 (in Chinese with English summary).

463 Fu L. K., Li Y., and Mill, R. R.: Podocarpaceae, in: Wu Z. Y., and Raven, P. H., (Eds.),

464 Flora of China, Science Press, Beijing, 4, 78–84, 1999.

465 Gale, J.: Availability of carbon dioxide for photosynthesis at high altitudes: theoretical  
466 considerations, *Ecology*, 53, 494–497, doi:10.2307/1934239, 1972.

467 Greenwood, D. G., Scarr, M. J., and Christophel, D. C.: Leaf stomatal frequency in the  
468 Australian tropical rain forest tree *Neolitseadealbata* (Lauraceae) as a proxy  
469 measure of atmospheric  $p\text{CO}_2$ , *Palaeogeography, Palaeoclimatology,*  
470 *Palaeoecology*, 196, 375–393, doi:10.1016/S0031-0182(03)00465-6, 2003.

471 Grein, M., Oehm, C., Konrad, W., Utescher, T., Kunzmann, L., and Roth-Nebelsick,  
472 A.: Atmospheric  $\text{CO}_2$  from the late Oligocene to early Miocene based on  
473 photosynthesis data and fossil leaf characteristics, *Palaeogeography,*  
474 *Palaeoclimatology, Palaeoecology*, 374, 41–51,  
475 doi:10.1016/j.palaeo.2012.12.025, 2013.

476 Henderiks, J., and Pagani, M.: Coccolithophore cell size and the Paleogene decline in  
477 atmospheric  $\text{CO}_2$ , *Earth and Planetary Science Letters* 269, 575–583,  
478 doi:10.1016/j.epsl.2008.03.016, 2008.

479 Hill, R. S., and Pole, M. S.: Leaf and shoot morphology of extant *Afrocarpus*, *Nageia*  
480 and *Retrophyllum* (Podocarpaceae) species, and species with similar leaf  
481 arrangement, from Tertiary sediments in Australasia, *Australian Systematic*  
482 *Botany*, 5, 337–358, doi:10.1071/SB9920337, 1992.

483 Hu, J. J., Xing, Y. W., Turkington, R., Jacques, F. M. B. Su, T., Huang, Y. J. and Zhou  
484 Z. K.: A new positive relationship between  $p\text{CO}_2$  and stomatal frequency in  
485 *Quercus guyavifolia* (Fagaceae): a potential proxy for palaeo- $\text{CO}_2$  levels, *Annals*

486 of Botany, 1–12, doi:10.1093/aob/mcv007, 2015.

487 Huang, C., Retallack, G. J., Wang, C., and Huang, Q.: Paleatmospheric pCO<sub>2</sub>  
488 fluctuations across the Cretaceous-Tertiary boundary recorded from paleosol  
489 carbonates in NE China, *Palaeogeography, Palaeoclimatology, Palaeoecology*,  
490 385, 95–105, doi.org/10.1016/j.palaeo.2013.01.005, 2013.

491 Jacques, F. M. B., Shi, G. L., Li, H. M., and Wang, W. M.: An Early-Middle Eocene  
492 Antarctic summer monsoon: Evidence of ‘fossil climates’, *Gondwana Research*,  
493 25, 1422–1428, doi:10.1016/j.gr.2012.08.007, 2014.

494 Jin, J. H., Qiu, J., Zhu, Y. A., and Kodrul, T. M.: First fossil record of the genus  
495 *Nageia* (Podocarpaceae) in South China and its phylogeographic implications,  
496 *Plant Systematics and Evolution*, 285, 159–163, doi:10.1007/s00606-010-0267-4,  
497 2010.

498 Jones, H. G.: *Plants and microclimate*, Cambridge UK Cambridge University Press,  
499 1–428, 1992.

500 Kato, Y., Fujinaga, K., and Suzuki, K.: Marine Os isotopic fluctuations in the Early  
501 Eocene greenhouse interval as recorded by metalliferous umbers from a Tertiary  
502 ophiolite in Japan, *Gondwana Research*, 20, 594–607,  
503 doi:10.1016/j.gr.2010.12.007, 2011.

504 Keating-Bitonti, C. R., Ivany, L. C., Affek, H. P., Douglas, P., and Samson, S. D.:  
505 Warm, not super-hot, temperatures in the early Eocene subtropics, *Geology* 39,  
506 771–774, doi: 10.1130/G32054.1, 2011.

507 Kimura, T., Ohana, T., and Mimoto, K.: Discovery of a podocarpaceous plant from



508 the Lower Cretaceous of Kochi Prefecture, in the outer zone of southwest Japan,  
509 Proceedings of the Japan Academy, ser. B, 64, 213–216, doi:10.2183/pjab.64.213,  
510 1988.

511 Koch, P. L., Zachos, J. C., and Gingerich, P. D.: Correlation between isotope records  
512 in marine and continental carbon reservoirs near the Palaeocene/Eocene  
513 boundary, *Nature*, 358, 319–322, doi:10.1038/358319a0, 1992.

514 Kouwenberg, L. L. R., McElwain J. C., Kürschner, W. M., Wagner, F., Beerling, S. J.,  
515 Mayle, F. E., and Visscher, H.: stomatal frequency adjustment of four conifer  
516 species to historical changes in atmospheric CO<sub>2</sub>, *American Journal of Botany*,  
517 90, 610–619, 2003.

518 Körner, Ch., and Cochrane, P. M.: Stomatal responses and water relations of  
519 *Eucalyptus pauciflora* in summer along an elevational gradient, *Oecologia*, 66,  
520 443–455, doi:10.1007/BF00378313, 1985.

521 Krassilov, V. A.: New coniferales from Lower Cretaceous of Primorye, *Botanical*  
522 *Journal*, 50, 1450–1455 (in Russia), 1965.

523 Kürschner, W. M., van der Burgh, J., Visscher, H., and Dilcher, D. L.: Oak leaves as  
524 biosensors of Late Neogene and Early Pleistocene paleoatmospheric CO<sub>2</sub>  
525 concentrations, *Marine Micropaleontology*, 27, 299–312,  
526 doi:10.1016/0377-8398(95)00067-4, 1996.

527 Kürschner, W. M., Wagner, F., Dilcher, D. L., and Visscher, H.: Using fossil leaves for  
528 the reconstruction of Cenozoic paleoatmospheric CO<sub>2</sub> concentrations, in:  
529 Gerhard, L. C., Harrison, W. E., Hanson, B. M., (Eds.), *Geological Perspectives*

530 of Global Climate Change, APPG Studies in Geology, 47, Tulsa, 169–189, 2001.

531 Kürschner, W. M., Kvaček, Z., and Dilcher, D. L.: The impact of Miocene  
532 atmospheric carbon dioxide fluctuations on climate and the evolution of  
533 terrestrial ecosystems, Proceedings of the National Academy of Sciences of the  
534 United States of America, 105, 449–453, doi:10.1073/pnas.0708588105, 2008.

535 Liu, X. Y., Gao, Q., and Jin, J. H.: Late Eocene leaves of *Nageia* Gaertner (section  
536 *Dammaroideae* Mill) from Maoming Basin, South China and their implications  
537 on phytogeography, Journal of Systematics and Evolution, 53, 297–307,  
538 doi:10.1111/jse.12133, 2015.

539 Lowenstein, T. K., and Demicco, R. V.: Elevated Eocene atmospheric CO<sub>2</sub> and its  
540 subsequent decline, Science, 313, 1928, doi:10.1126/science.1129555, 2006.

541 McElwain, J. C.: Do fossil plants signal palaeoatmospheric carbon dioxide  
542 concentration in the geological past, Philosophical Transactions of the Royal  
543 Society, Lond B, 353, 83–96, doi:10.1098/rstb.1998.0193, 1998.

544 McElwain, J. C., and Chaloner, W. G.: Stomatal density and index of fossil plants  
545 track atmospheric carbon dioxide in the Palaeozoic, Annals of Botany, 76,  
546 389–395, doi:10.1006/anbo.1995.1112, 1995.

547 McElwain, J. C., and Chaloner, W. G.: The fossil cuticle as a skeletal record of  
548 environmental changes, Palaios, 11, 376–388, doi: 10.2307/3515247, 1996.

549 Mill, R. R.: A new combination in *Nageia* (Podocarpaceae): Novon, 9, 77–78, 1999.

550 Mill, R. R.: A new sectional combination in *Nageia* Gaertn (Podocarpaceae),  
551 Edinburgh Journal of Botany, 58, 499–501, doi:10.1017/S0960428601000804,

552 2001.

553 Maxbauer, D. P., Royer, D. L., and LePage, B. A.: High Arctic forests during the  
554 middle Eocene supported by moderate levels of atmospheric CO<sub>2</sub>, *Geology*, 42,  
555 1027–1030, doi:10.1130/G36014.1, 2014.

556 Moran, K., Backman, J., Brinkhuis, H., Clemens, S. C., Cronin, T., Dickens, G. R.,  
557 Eynaud, F., Gattacceca, J., Jakobsson, M., Jordan, R. W., Kaminski, M., King, J.,  
558 Koc, N., Krylov, A., Martinez, N., Matthiessen, J., McInroy, D., Moore, T.C.,  
559 Onodera, J., O'Regan, M., Päike, H., Rea, B., Rio, D., Sakamoto, T., Smith, D.  
560 C., Stein, R., St John, K., Suto, I., Suzuki, N., Takahashi, K., Watanabe, M.,  
561 Yamamoto, M., Farrell, J., Frank, M., Kubik, P., Jokat, W., and Kristoffersen, Y.:  
562 The Cenozoic palaeoenvironment of the Arctic Ocean, *Nature*, 441, 601–605,  
563 doi:10.1038/nature04800, 2006.

564 Nordt, L., Atchley, S., and Dworkin, S. I.: Paleosol barometer indicates extreme  
565 fluctuations in atmospheric CO<sub>2</sub> across the Cretaceous-Tertiary boundary,  
566 *Geology*, 30, 703–706, doi:10.1130/0091-7613(2002)030<0703:PBIEFI>  
567 2.0.CO;2, 2002.

568 Pagani, M., Arthur, M. A., and Freeman, K. H.: Miocene evolution of atmospheric  
569 carbon dioxide, *Paleoceanography*, 14, doi:10.1029/1999PA900006, 273–292,  
570 1999.

571 Pagani, M., Zachos, J. C., Freeman, K. H., Tipple, B., and Bohaty, S.: Marked decline  
572 in atmospheric carbon dioxide concentrations during the Paleocene, *Science*, 309,  
573 600–603, doi:10.1126/science.1110063, 2005.

574 Pearson, P. N., Foster, G. L., and Wade, B. S.: Atmospheric carbon dioxide through the  
575 Eocene-Oligocene climate transition, *Nature*, 461, 1110–1113,  
576 doi:10.1038/nature08447, 2009.

577 Petit, J. R., Jouzel, J., Raynaud, D., Barkov, N. I., Barnola, J.-M., Basile, I., Bender,  
578 M., Chappellaz, J., Davis, M., Delaygue, G., Delmotte, M., Kotlyakov, V. M.,  
579 Legrand, M., Lipenkov, V. Y., Lorius, C., PÉpin, L., Ritz, C., Saltzman, E., and  
580 Stievenard, M.: Climate and atmospheric history of the past 420,000 years from  
581 the Vostokicecore, Antarctica, *Nature*, 399, 429–436, doi:10.1038/20859, 1999.

582 Pieter, T., and Keeling, R.: Recent monthly average Mauna Loa CO<sub>2</sub>, NOAA/ESRL,  
583 www.esrl.noaa.gov/gmd/ccgg/trends/ (accessed March 2015), 2015.

584 Poole, I., and Kürschner, W. M.: Stomatal density and index: the practice, in: Jones,  
585 T.P., and Rowe, N.P., (Eds.), *Fossil Plants and Spores: Modern Techniques*,  
586 Geological Society, London, 257–260, 1999.

587 Retallack, G. J.: A 300-million-year record of atmospheric carbon dioxide from fossil  
588 plant cuticles, *Nature*, 411, 287–290, doi:10.1038/35077041, 2001.

589 Retallack, G. J.: Greenhouse crises of the past 300 million years, *Geological Society*  
590 *of America Bulletin*, 121, 1441–1455, doi:10.1130/B26341.1, 2009a.

591 Retallack, G. J.: Refining a pedogenic-carbonate CO<sub>2</sub> paleobarometer to quantify a  
592 Middle Miocene greenhouse spike, *Palaeogeography, Palaeoclimatology,*  
593 *Palaeoecology*, 281, 57–65, doi:10.1016/j.palaeo.2009.07.011, 2009b.

594 Roth-Nebelsick, A., Grein, M., Utescher, T., and Konrad, W.: Stomatal pore length  
595 change in leaves of *Eotrigonobalanus furcinervis* (Fagaceae) from the Late

596 Eocene to the Latest Oligocene and its impact on gas exchange and CO<sub>2</sub>  
597 reconstruction, *Review of Palaeobotany and Palynology*, 174, 106–112,  
598 doi:10.1016/j.revpalbo.2012.01.001, 2012.

599 Roth-Nebelsick, A., Oehm, C., Grein, M., Utescher, T., Kunzmann, L., Friedrich, J.-P.,  
600 and Konrad, W.: Stomatal density and index data of *Platanus neptuni* leaf fossils  
601 and their evaluation as a CO<sub>2</sub> proxy for the Oligocene, *Review of Palaeobotany*  
602 and *Palynology*, 206, 1–9, doi:10.1016/j.revpalbo.2014.03.001, 2014.

603 Royer, D. L.: Stomatal density and stomatal index as indicators of paleoatmospheric  
604 CO<sub>2</sub> concentration, *Review of Palaeobotany and Palynology*, 114, 1–28,  
605 doi:10.1016/S0034-6667(00)00074-9, 2001.

606 Royer, D. L.: Estimating Latest Cretaceous and Tertiary atmospheric CO<sub>2</sub> from  
607 stomatal indices, in: Wing, S. L., Gingerich, P. D., Schmitz, B., and Thomas, E.,  
608 (Eds.), *Causes and Consequences of Globally Warm Climates in the Early*  
609 *Paleocene*, Geological Society of America Special Paper, 79–93, 2003.

610 Royer, D. L.: CO<sub>2</sub>-forced climate thresholds during the Phanerozoic, *Geochimica et*  
611 *Cosmochimica Acta*, 70, 5665–5675, doi:10.1016/j.gca.2005.11.031, 2006.

612 Royer, D. L., Wing, S. L., Beerling, D. J., Jolley, D. W., Koch, P. L., Hickey, L. J., and  
613 Berner, R. A.: Paleobotanical evidence for near present-day levels of atmospheric  
614 CO<sub>2</sub> during part of the Tertiary, *Science*, 292, 2310–2313,  
615 doi:10.1126/science.292.5525.2310, 2001.

616 Rundgren, M., and Beerling, D. J.: A Holocene CO<sub>2</sub> record from the stomatal index of  
617 subfossil *Salix herbacea* L. leaves from northern Sweden, *The Holocene*, 9,

618 509–513, doi:10.1191/095968399677717287, 1999.

619 Seki, O, Foster, G. L., Schmidt, D. N., Mackensen, A., Kawamura, K., and Pancost, R.  
620 D.: Alkenone and boron-based Pliocene  $p\text{CO}_2$  records, *Earth and Planetary*  
621 *Science Letters*, 292, 201–211, doi:10.1016/j.epsl.2010.01.037, 2010.

622 Sinha, A., and Stott, L. D.: New atmospheric  $p\text{CO}_2$  estimates from paleosols during  
623 the late Paleocene/early Eocene global warming interval, *Global and Planetary*  
624 *Change*, 9, 297–307, doi:10.1016/0921-8181(94)00010-7, 1994,

625 Smith, R. Y., Greenwood, D. R., and Basinger, J.F.: Estimating paleoatmospheric  
626  $p\text{CO}_2$  during the Early Eocene Climatic Optimum from stomatal frequency of  
627 *Ginkgo*, Okanagan Highlands, British Columbia, Canada, *Palaeogeography,*  
628 *Palaeoclimatology, Palaeoecology*, 293, 120–131,  
629 doi:10.1016/j.palaeo.2010.05.006, 2010.

630 Spicer, A. R., Herman, A. B., Liao, W. B., Spicer, T. E. V., Kodrul, T. M., Yang, J., and  
631 Jin, J. H.: Cool tropics in the middle Eocene: Evidence from the Changchang  
632 Flora, Hainan Island, China, *Palaeogeography, Palaeoclimatology, Palaeoecology*,  
633 412, 1–16, doi:10.1016/j.palaeo.2014.07.011, 2014.

634 Stott, L. D.: Higher temperatures and lower oceanic  $p\text{CO}_2$ : A climate enigma at the  
635 end of the Paleocene Epoch, *Paleoceanography*, 7, 395–404,  
636 doi:10.1029/92PA01183, 1992.

637 Stults, D. Z., Wagner-Cremer, F., and Axsmith, B. J.: Atmospheric paleo- $\text{CO}_2$   
638 estimates based on *Taxodium distichum* (Cupressaceae) fossils from the Miocene  
639 and Pliocene of Eastern North America, *Palaeogeography Palaeoclimatology*

640 Palaeoecology, 309, 327–332, doi:10.1016/j.palaeo.2011.06.017, 2011.

641 Sun, B. N., Ding, S. T., Wu, J. Y., Dong, C., Xie, S. P., and Lin, Z. C.: Carbon isotope  
642 and stomatal data of Late Pliocene Betulaceae leaves from SW China:  
643 Implications for palaeoatmospheric CO<sub>2</sub>-levels, Turkish Journal of Earth  
644 Sciences, 21, 237–250, doi:10.3906/yer-1003-42, 2012.

645 Sun, T. X.: Cuticle micromorphology of *Nageia*, Journal of Wuhan Botanical  
646 Research, 26, 554–560, doi:10.3969/j.issn.2095-0837.2008.06.002, 2008 (in  
647 Chinese with English abstract).

648 Tripathi, A. K., Roberts, C. D., and Eagle, R. A.: Coupling of CO<sub>2</sub> and ice sheet  
649 stability over major climate transitions of the last 20 million years, Science, 326,  
650 1394–1397, doi:10.1126/science.1178296, 2009.

651 Van der Burgh, J., Visscher, H., Dilcher, D. L., and Kürschner, W. M.:  
652 Paleoatmospheric signatures in Neogene fossil leaves, Science, 260, 1788–1790,  
653 doi:10.1126/science.260.5115.1788, 1993.

654 Wang, J. D., Li, H. M., and Zhu Z. Y.: Magnetostratigraphy of Tertiary rocks from  
655 Maoming Basin, Guangdong province, China, Chinese Journal of Geochemistry,  
656 13, 165–175, doi:10.1007/BF02838516, 1994.

657 Walker, J. D., and Geissman, J. W.: Geologic Time Scale, Geological Society of  
658 America, doi:10.1130/2009.CTS004R2C, 2009.

659 Wing, S. L., Harrington, G. J., Smith, F. A., Bloch, J. I., Boyer, D. M., and Freeman, K.  
660 H.: Transient floral change and rapid global warming at the Paleocene-Eocene  
661 boundary, Science, 310, 993–996, doi:10.1126/science.1116913, 2005.

662 Woodward, F. I.: Ecophysiological studies on the shrub *Vaccinium myrtillus* L. taken  
663 from a wide altitudinal range, *Oecologia*, 70, 580–586, doi:10.1007/BF00379908,  
664 1986.

665 Woodward, F. I.: Stomatal numbers are sensitive to increases in CO<sub>2</sub> concentration  
666 from pre-industrial levels, *Nature*, 327, 617–618, doi:10.1038/327617a0, 1987.

667 Woodward, F. I., and Bazzaz, F. A.: The responses of stomatal density to CO<sub>2</sub> partial  
668 pressure, *Journal of Experimental Botany*, 39, 1771–1781,  
669 doi:10.1093/jxb/39.12.1771, 1988.

670 Yang, J. J., Qi, G. F., and Xu, R. H.: Studies on fossil woods excavated from the Dabie  
671 mountains, *Scientia Silvae Sinicae*, 26, 379–386, 1990 (in Chinese with English  
672 abstract).

673 Ye, M. N.: On the preparation methods of fossil cuticle. *Palaeontological Society of*  
674 *China* (Ed.), Selected papers of the 12th Annual conference of the  
675 *Palaeontological Society of China*, Science Press, Beijing, 170–179, 1981 (in  
676 Chinese).

677 Zachos, J., Pagani, M., Sloan, L., Thomas, E., and Billups, K.: Trends, rhythms,  
678 aberrations in global climate 65 Ma to present, *Science*, 292, 686–693,  
679 doi:10.1126/science.1059412, 2001.

680 Zachos, J., Dickens, G. R. and Zeebe, R. E.: An early Cenozoic perspective on  
681 greenhouse warming and carbon-cycle dynamics, *Nature*, 451, 279–283,  
682 doi:10.1038/nature06588, 2008.

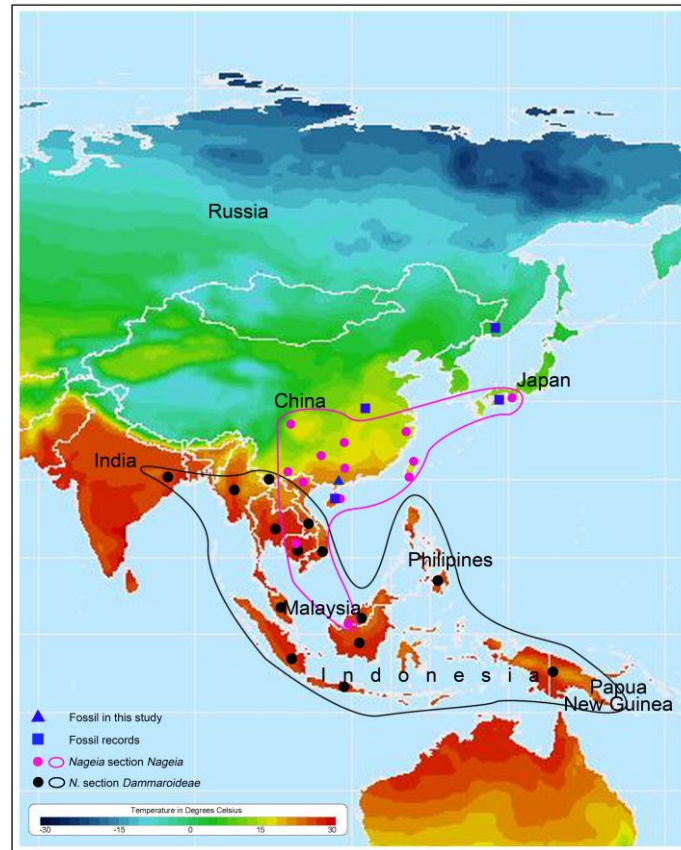


683

684 Figure 1. Map showing the distribution of extant and fossil *Nageia* and their mean annual

685 temperature (Modified after the map from

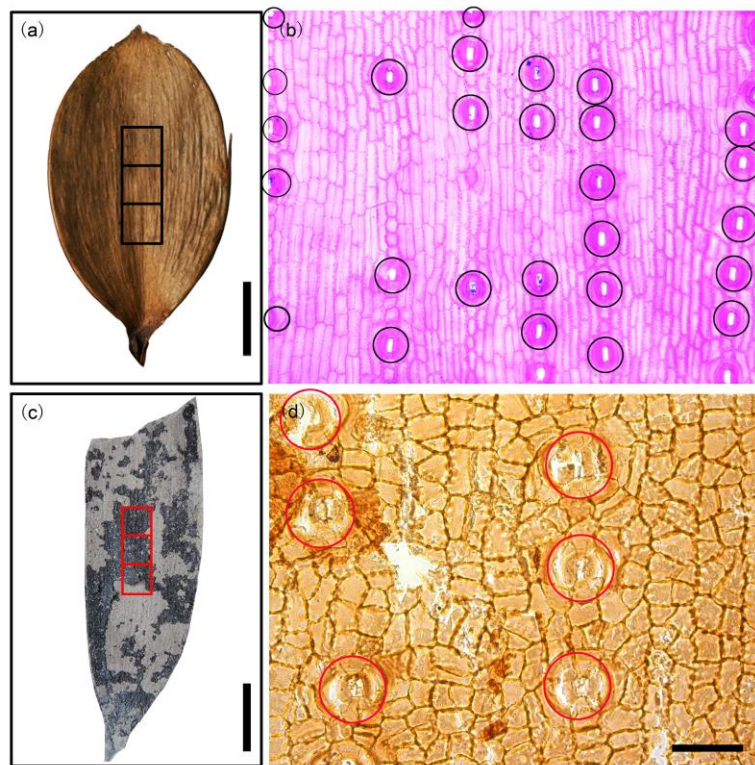
686 <http://www.sage.wisc.edu/atlas/maps.php?datasetid=35&includerelatedlinks=1&dataset=35>).



687

688

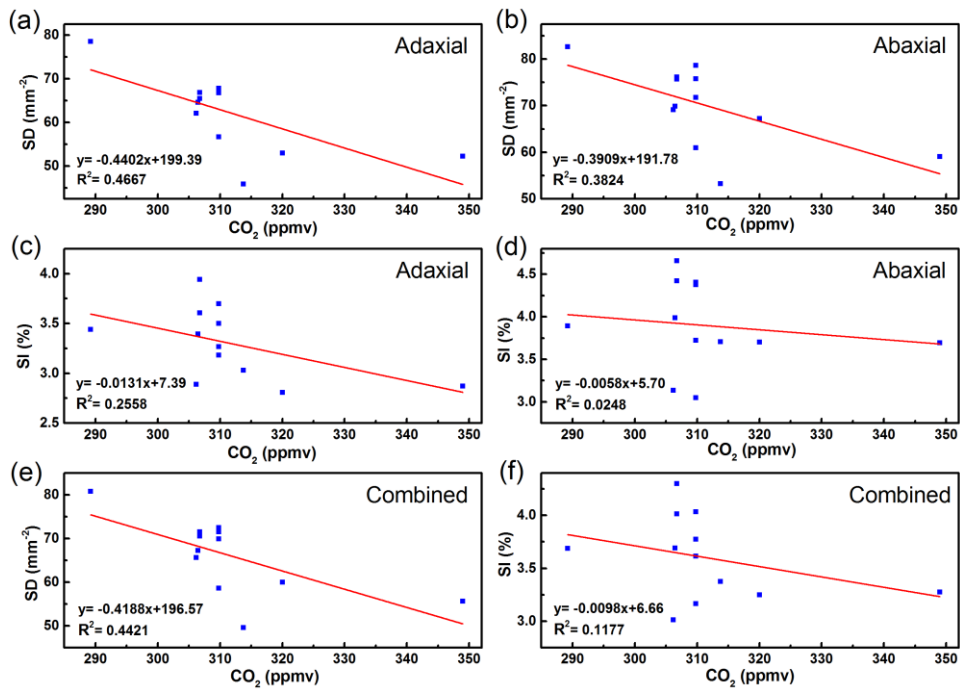
689 Figure 2. Sampling areas and counting rules are shown. (a) *Nageia motleyi* (Parl.) De Laub.leaf.  
690 Black squares in the middle of the leaf show the sampling areas for preparing the cuticles. (b) The  
691 abaxial side of the cuticle from *N. motleyi* leaf. Black circles show the counted stomatal  
692 complexes. (c) *N. maomingensis* Jin et Liu. Red squares in the middle of the leaf indicate the  
693 sampling areas. (d) The abaxial side of the fossil cuticle. Red circles show the counted stomatal  
694 complexes. Scale bars: (a) and (c) = 1 cm; (b) and (d) = 50  $\mu$ m.



695

696

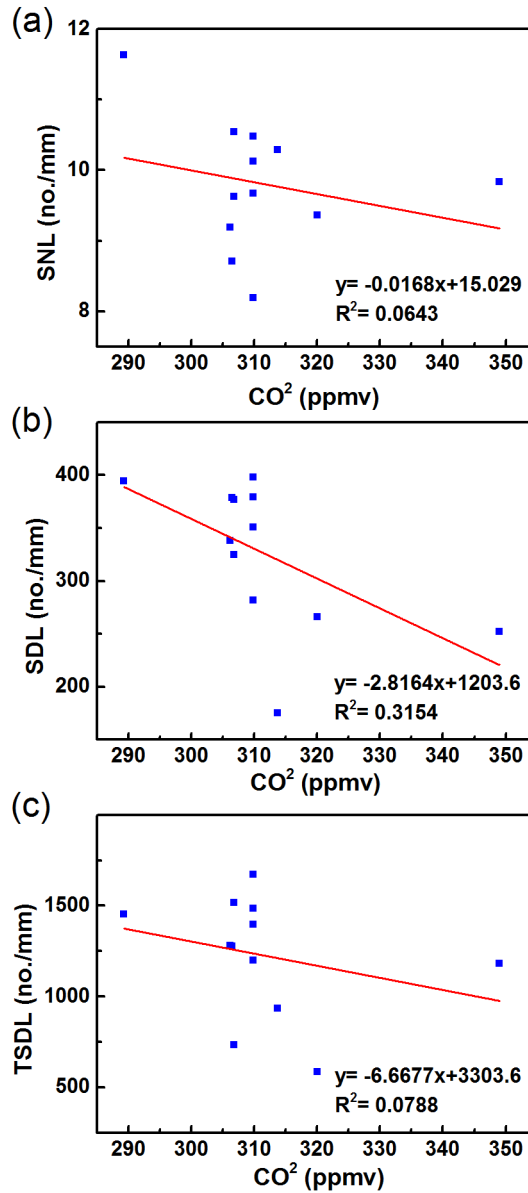
697 Figure 3. Correlation between SD and SI versus CO<sub>2</sub> concentration for modern *Nageia motleyi*. (a)  
 698 Trends of SD with CO<sub>2</sub> concentration for the adaxial surface. (b) Trends of SD with CO<sub>2</sub>  
 699 concentration for the abaxial surface. (c) Trends of SI with CO<sub>2</sub> concentration for the adaxial  
 700 surface. (d) Trends of SI with CO<sub>2</sub> concentration for the abaxial surface. (e) Trends of SD with  
 701 CO<sub>2</sub> concentration for the combined data of both leaf surfaces. (f) Trends of SI with CO<sub>2</sub>  
 702 concentration for the combined data of both leaf surfaces.



703

704

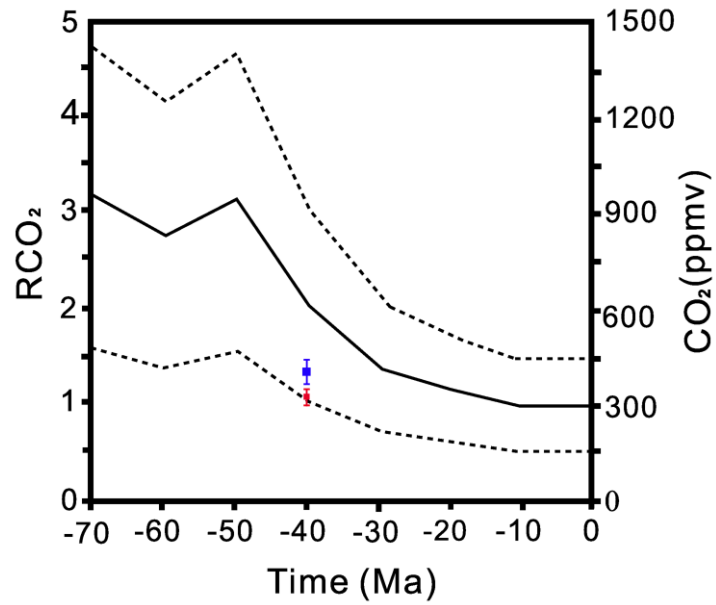
705 Figure 4. Correlation between SNL, SDL and TSDL versus CO<sub>2</sub> concentration for modern *Nageia*  
 706 *motleyi*. (a) Trends of SNL with CO<sub>2</sub> concentration for the adaxial surface. (b) Trends of SDL with  
 707 CO<sub>2</sub> concentration for the adaxial surface. (c) Trends of TSDL with CO<sub>2</sub> concentration for the  
 708 adaxial surface.



709

710

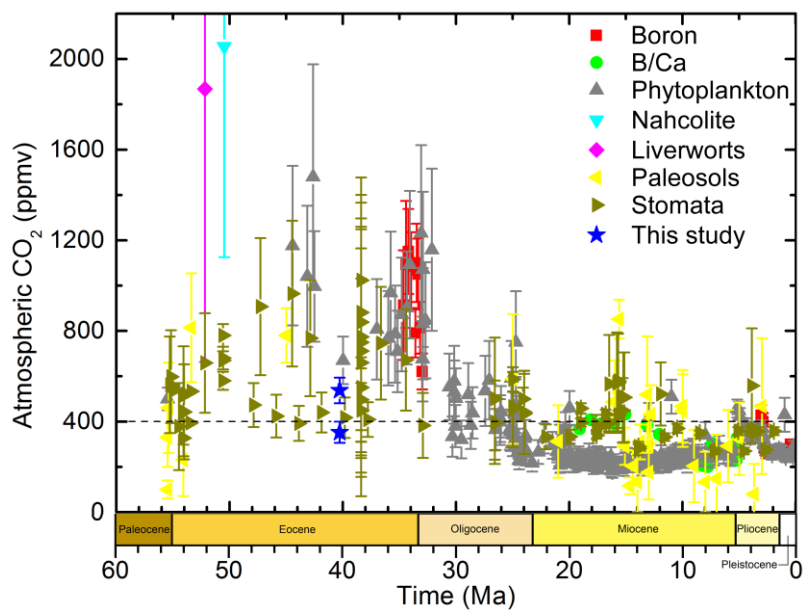
711 Figure 5. The pCO<sub>2</sub> reconstruction results and extant CO<sub>2</sub> concentrations are projected onto the  
712 long-term carbon cycle model (GEOCARB III; Berner and Kothaval á 2001). The pCO<sub>2</sub> results  
713 based on the regression approach and stomatal ratio method are represented by red and blue  
714 squares, respectively.



715

716

717 Figure 6. Atmospheric CO<sub>2</sub> estimates from proxies over the past 60 million years. The horizontal  
718 dashed line indicates monthly atmospheric CO<sub>2</sub> concentration for March 2015 at Mauna Loa,  
719 Hawaii (401.5 ppmv) (Pieter and Keeling, 2015). The vertical lines show the error bars. The data  
720 are from the supporting data of Beerling and Royer (2011) and references in Table 9. The lower  
721 blue star shows the reconstructed result based on the regression approach. The higher one presents  
722 the result of stomatal ratio method.



723

724 Table 1. Modern *Nageia motleyi* (Parl.) De Laub samples and atmospheric CO<sub>2</sub> values of their collection dates from ice core data (Brown, 2010).

725

Herbarium	Collection number	Collecting locality	Collectors	Number of leaf samples	Collection date	CO <sub>2</sub> (ppmv)
LE	No. 2649	Malaysia	Beccari, O.	1	1868	289.23
A/GH	No. bb. 17229	150 m, Riau on Ond. Karimon, Archipel. Ind.	Neth. Ind. For. Service	2	1932	306.19
A/GH	No. bb. 18328	5 m, Z. O. afd. v. Borneo Tidoengsche Landen, Archipel. Ind.	Neth. Ind. For. Service	2	1934	306.46
A/GH	No. bb. 21151	500 m, Z. O. afd. Borneo, Poeroek Tjahoe Tahoedjan, Archipel. Ind.	Neth. Ind. For. Service	2	1936	306.76
KEP	No. 30887	Kata Tinggi, Johor, Malaysia	Corner, E.J.H.	1	1936	306.76
KEP	No. 57329	Batang Padang, Perak, Malaysia	Unkonwn	2	1947	309.82
KEP	No. 57330	Batang Padang, Perak, Malaysia	Unkonwn	2	1947	309.82
KEP	No. 55897	Batang Padang, Perak, Malaysia	Unkonwn	2	1947	309.82
KEP	No. 61064	Batang Padang, Perak, Malaysia	Syed Woh	2	1947	309.82
E	No. bb. 40798	51 m, Kuala Trengganu-Besut Road, Bukit Bintang Block, Gunong Tebu Forest reserve, Malaysia	Sinclair, J. and Kiah bin, Salleh	2	1955	313.73
KEP	No. 80548	Gombak, Selangor, Malaysia	Rahim	1	1965	320.04
KEP	No. 33343	Jelebu, Negeri Sembilan, Malaysia	Yap, S.K.	2	1987	348.98

Note: A/GH—Harvard University Herbarium, Harvard University, 22 Divinity Avenue, Cambridge, Massachusetts 02138, USA ([www.huh.harvard.edu](http://www.huh.harvard.edu)).

E—The Herbarium of Royal Botanic Garden, Edinburgh EH3 5LR, Scotland, UK ([www.rbge.org.uk](http://www.rbge.org.uk)).

LE—The Herbarium of the V.L. Komarov Botanical Institute of the Russian Academy of Sciences, Prof. Popov Street 2, Saint Petersburg 197376, Russia ([www.binran.ru](http://www.binran.ru)).

KEP—Kepong Herbarium, Forest Research Institute Malaysia, 52109 Kepong, Selangor, Malaysia (<http://www.frim.gov.my/>).

726 Table 2. Summary of stomatal parameters of the adaxial surface from modern *Nageia motleyi* (Parl.) De Laub.

Collection number	Collection date	CO <sub>2</sub> (ppmv)	SD (mm <sup>-2</sup> )					SI (%)				
			<i>x</i>	$\sigma$	s.e.	t*s.e.	n	<i>x</i>	$\sigma$	s.e.	t*s.e.	n
No.2649	1868	289.23	78.60	15.44	1.41	2.76	120	3.44	0.66	0.06	0.12	120
No.bb.17229	1932	306.19	62.14	17.20	1.78	3.50	93	2.89	0.68	0.07	0.14	93
No.bb.18328	1934	306.46	64.57	15.05	1.58	3.11	90	3.39	1.01	0.11	0.21	90
No.bb.21151	1936	306.76	65.45	11.14	1.17	2.30	90	3.94	0.74	0.08	0.15	90
No.SFN30887	1936	306.76	66.90	16.10	1.27	2.49	161	3.61	0.92	0.07	0.14	161
No.61064	1947	309.82	56.71	16.81	1.95	3.83	74	3.27	1.26	0.15	0.29	74
No.57330	1947	309.82	67.37	15.97	2.04	4.01	61	3.70	0.82	0.10	0.20	61
No.57329	1947	309.82	67.85	15.61	1.70	3.34	84	3.50	0.90	0.10	0.20	84
No.55897	1947	309.82	66.74	14.10	1.78	3.48	63	3.18	0.66	0.08	0.16	63
No.40798	1955	313.73	45.89	13.81	1.12	2.20	151	3.03	0.87	0.07	0.14	151
No.KEP80548	1965	320.04	52.94	11.25	0.85	1.67	175	2.81	0.61	0.05	0.09	175
No.FRI33343	1987	348.98	52.25	12.05	0.77	1.51	242	2.87	0.69	0.04	0.09	242
Mean	—	—	62.28	14.54	1.45	2.85	117	3.30	0.52	0.08	0.16	117

Note: *x*—mean;  $\sigma$ —standard deviation; s.e. —standard error of mean; n— numbers of photos counts (40 $\times$ ); t\*s.e.— 95% confidence interval.



727 Table 3. Summary of stomatal parameters of the abaxial surface from modern *Nageia motleyi* (Parl.) De Laub.

Collection number	Collection date	CO <sub>2</sub> (ppmv)	SD (mm <sup>-2</sup> )					SI (%)				
			<i>x</i>	$\sigma$	s.e.	t*s.e.	n	<i>x</i>	$\sigma$	s.e.	t*s.e.	n
No.2649	1868	289.23	82.71	12.23	1.02	2.00	144	3.89	0.58	0.05	0.09	144
No.bb.17229	1932	306.19	69.16	14.23	1.48	2.90	93	3.13	0.58	0.06	0.12	93
No.bb.18328	1934	306.46	69.92	14.38	1.52	2.97	90	3.99	1.08	0.11	0.22	90
No.bb.21151	1936	306.76	75.68	15.74	1.66	3.25	90	4.66	0.88	0.09	0.18	90
No.SFN30887	1936	306.76	76.18	12.51	0.99	1.93	161	4.42	0.89	0.07	0.14	161
No.61064	1947	309.82	60.93	11.02	1.39	2.72	63	3.05	0.62	0.08	0.15	63
No.57330	1947	309.82	75.82	14.14	1.82	3.58	60	4.38	0.84	0.11	0.21	60
No.57329	1947	309.82	71.74	16.84	1.75	3.42	93	3.72	0.62	0.06	0.13	93
No.55897	1947	309.82	78.63	13.41	1.75	3.42	59	4.41	1.00	0.13	0.26	59
No.40798	1955	313.73	53.22	13.88	1.12	2.19	155	3.71	0.93	0.07	0.15	155
No.KEP80548	1965	320.04	67.22	13.97	1.07	2.09	171	3.70	0.80	0.06	0.12	171
No.FRI33343	1987	348.98	59.09	12.10	0.79	1.55	233	3.69	0.86	0.06	0.11	233
Mean	—	—	70.03	13.70	1.36	2.67	118	3.90	0.81	0.08	0.16	118

Note: *x*—mean;  $\sigma$ —standard deviation; s.e. —standard error of mean; n— numbers of photos counts (40×); t\*s.e.— 95% confidence interval.

729 Table 4. Summary of stomatal parameters of the combined data of the adaxial and abaxial surfaces from modern *Nageia motleyi* (Parl.) De Laub.

Collection number	Collection date	CO <sub>2</sub> (ppmv)	SD (mm <sup>-2</sup> )					SI (%)				
			<i>x</i>	$\sigma$	s.e.	t*s.e.	n	<i>x</i>	$\sigma$	s.e.	t*s.e.	n
No.2649	1868	289.23	80.84	13.74	0.85	1.66	264	3.69	0.66	0.04	0.08	264
No.bb.17229	1932	306.19	65.65	16.13	1.18	2.32	186	3.01	0.64	0.05	0.09	186
No.bb.18328	1934	306.46	67.24	14.92	1.11	2.18	180	3.69	1.08	0.08	0.16	180
No.bb.21151	1936	306.76	70.57	14.53	1.08	2.12	180	4.30	0.89	0.07	0.13	180
No.SFN30887	1936	306.76	71.54	15.12	0.84	1.65	322	4.01	0.99	0.05	0.11	322
No.61064	1947	309.82	58.65	14.54	1.24	2.43	137	3.17	1.02	0.09	0.17	137
No.57330	1947	309.82	71.56	15.61	1.42	2.78	121	4.03	0.89	0.08	0.16	121
No.57329	1947	309.82	69.90	16.33	1.23	2.41	177	3.62	0.77	0.06	0.11	177
No.55897	1947	309.82	72.49	14.95	1.35	2.65	122	3.77	1.04	0.09	0.18	122
No.40798	1955	313.73	49.60	14.31	0.82	1.60	306	3.37	0.96	0.05	0.11	306
No.KEP80548	1965	320.04	60.00	14.53	0.78	1.53	346	3.25	0.84	0.05	0.09	346
No.FRI33343	1987	348.98	55.61	12.53	0.58	1.13	475	3.28	0.88	0.04	0.08	475
Mean	—	—	66.14	14.77	1.04	2.08	235	3.60	0.89	0.06	0.12	235

*Note:* *x*—mean;  $\sigma$ —standard deviation; s.e. —standard error of mean; n— numbers of photos counts (40 $\times$ ); t\*s.e.— 95% confidence interval.

731 Table 5. Summary of stomatal parameters from modern *Nageia motleyi* (Parl.) De Laub (Kouwenberg et al., 2003).

Collection number	Collection date	CO <sub>2</sub> (ppmv)	SNL	SDL	TSDL	n
No.2649	1868	289.23	11.64	394.38	1455.10	264
No.bb.17229	1932	306.19	9.19	337.98	1280.12	186
No.bb.18328	1934	306.46	8.71	378.92	1277.63	180
No.bb.21151	1936	306.76	9.62	376.93	1517.21	180
No.SFN30887	1936	306.76	10.55	325.08	735.38	240
No.61064	1947	309.82	8.19	282.04	1200.66	133
No.57330	1947	309.82	9.67	397.83	1397.33	119
No.57329	1947	309.82	10.13	350.98	1672.50	176
No.55897	1947	309.82	10.48	379.06	1486.13	122
No.40798	1955	313.73	10.29	175.14	933.85	305
No.KEP80548	1965	320.04	9.36	266.16	585.72	263
No.FRI33343	1987	348.98	9.84	252.20	1181.51	125
Mean	–	–	9.81	326.39	1226.93	191

732

733

734

735 Table 6. Summary of stomatal parameters of the adaxial surface of fossil *Nageia* and pCO<sub>2</sub> [*C*<sub>(f)</sub>] estimates results.

Species	Age	SD (mm <sup>-2</sup> )				SI (%)				SR		pCO <sub>2</sub> (ppmv)		<i>C</i> <sub>(f)</sub> (ppmv)	
		<i>x</i>	$\sigma$	s.e.	n	<i>x</i>	$\sigma$	s.e.	n	<i>x</i>	t*s.e	<i>x</i>	t*s.e	<i>x</i>	t*s.e
MMJ1-001	Late Eocene	52.5	17.1	3.1	30	2.08	0.7	0.1	30	1.35	0.19	333.6	13.9	412.1	62.0
MMJ2-003	Late Eocene	42.3	12.9	2.4	30	1.80	0.6	0.1	30	1.75	0.39	356.8	10.5	536.1	126.2
MMJ2-004	Late Eocene	39.9	13.6	2.5	30	1.66	0.6	0.1	30	1.81	0.32	362.4	11.0	554.3	101.9
MMJ3-003a	Late Eocene	43.2	17.7	3.2	30	1.67	0.7	0.1	30	1.84	0.43	354.8	14.4	564.6	135.7
Mean	Late Eocene	44.5	16.3	1.5	120	1.80	0.7	0.1	120	1.69	0.18	351.9	6.6	516.8	56.5

*Note:* *x*—mean;  $\sigma$ —standard deviation; s.e. —standard error of mean; n— numbers of photos counts (400×); t\*s.e.— 95% confidence interval. pCO<sub>2</sub>— the result based the regression approach; *C*<sub>(f)</sub>— the result based on the stomatal method.

736

737

738 Table 7. Summary of stomatal parameters of the abaxial surface of fossil *Nageia* and pCO<sub>2</sub> [*C<sub>f</sub>*] estimates results.

Species	Age	SD (mm <sup>-2</sup> )				SI (%)				SR		pCO <sub>2</sub> (ppmv)		<i>C<sub>f</sub></i> (ppmv)	
		<i>x</i>	$\sigma$	s.e.	n	<i>x</i>	$\sigma$	s.e.	n	<i>x</i>	t*s.e	<i>x</i>	t*s.e	<i>x</i>	t*s.e
MMJ1-001	Late Eocene	47.7	17.7	3.2	30	2.11	0.8	0.2	30	1.66	0.23	368.6	16.2	515.6	72.3
MMJ2-003	Late Eocene	50.9	18.3	3.3	30	2.12	0.8	0.1	30	1.57	0.23	360.9	16.6	486.0	70.7
MMJ2-004	Late Eocene	48.2	15.8	2.9	30	2.14	0.7	0.1	30	1.63	0.25	367.4	14.5	504.6	77.3
MMJ3-003a	Late Eocene	48.9	12.6	2.7	22	1.85	0.5	0.1	22	1.52	0.19	365.4	13.5	472.3	59.0
Mean	Late Eocene	48.9	16.2	1.5	112	2.07	0.7	0.1	112	1.60	0.11	365.6	7.6	496.1	35.7

Note: *x*—mean;  $\sigma$ —standard deviation; s.e. —standard error of mean; n— numbers of photos counts (400×); t\*s.e.— 95% confidence interval. pCO<sub>2</sub>— the result based the regression approach; *C<sub>f</sub>*— the result based on the stomatal method.

739

740 Table 8. Summary of stomatal parameters of the combined data of the adaxial and abaxial surfaces of fossil *Nageia* and pCO<sub>2</sub> [*C*<sub>(f)</sub>] estimates  
 741 results.

Species	Age	SD (mm <sup>-2</sup> )				SI (%)				SR		pCO <sub>2</sub> (ppmv)		<i>C</i> <sub>(f)</sub> (ppmv)	
		<i>x</i>	$\sigma$	s.e.	n	<i>x</i>	$\sigma$	s.e.	n	<i>x</i>	t*s.e	<i>x</i>	t*s.e	<i>x</i>	t*s.e
MMJ1-001	Late Eocene	50.1	17.5	2.3	60	2.09	0.8	0.1	60	1.50	0.15	349.7	10.6	471.2	47.8
MMJ2-003	Late Eocene	46.5	16.3	2.1	60	1.96	0.7	0.1	60	1.67	0.24	358.3	9.8	524.1	75.7
MMJ2-004	Late Eocene	44.0	15.8	2.0	60	1.90	0.7	0.1	60	1.73	0.17	364.3	9.5	542.9	52.6
MMJ3-003a	Late Eocene	45.6	16.1	2.2	52	1.75	0.6	0.1	52	1.73	0.28	360.5	10.4	544.6	88.3
Mean	Late Eocene	46.6	16.4	1.1	232	1.93	0.7	0.1	232	1.66	0.11	358.1	5.0	519.9	35.0

*Note:* *x*—mean;  $\sigma$ —standard deviation; s.e. —standard error of mean; n— numbers of photos counts (400×); t\*s.e.— 95% confidence interval. pCO<sub>2</sub>— the result based the regression approach; *C*<sub>(f)</sub>— the result based on the stomatal method.

742

743 Table 9. pCO<sub>2</sub> estimates proxies and corresponding references.

Proxies	References
Boron	Pearson et al., 2009; Seki et al., 2010
B/Ca	Tripathi et al., 2009
Phytoplankton	Freeman and Hayes, 1992; Stott, 1992; Pagani et al., 1999, 2005; Henderiks and Pagani, 2008; Seki et al., 2010
Nahcolite	Lowenstein and Demicco, 2006
Liverworts	Fletcher et al., 2008
Paleosols	Cerling, 1992; Koch et al., 1992; Ekart et al., 1999; Royer et al., 2001; Nordt et al., 2002; Retallack, 2009b; Huang et al. 2013
Stomata	Van der Burgh et al., 1993; Kürschner et al., 1996, 2001, 2008; McElwain, 1998; Royer et al., 2001, 2003; Greenwood et al., 2003; Beerling et al., 2009; Retallack, 2009a; Smith et al., 2010; Doria et al., 2011; Roth-Nebelsick et al., 2012; 2014; Grein et al., 2013; Maxbauer et al., 2014

744